

Reduced order modeling and analysis of the human complement system

Adithya Sagar, Wei Dai[#], Mason Minot[#], and Jeffrey D. Varner*

School of Chemical and Biomolecular Engineering

Cornell University, Ithaca NY 14853

Running Title: A reduced order model of complement

To be submitted: *PLoS ONE*

Denotes equal contribution

*Corresponding author:

Jeffrey D. Varner,

Professor, School of Chemical and Biomolecular Engineering,

244 Olin Hall, Cornell University, Ithaca NY, 14853

Email: jdv27@cornell.edu

Phone: (607) 255 - 4258

Fax: (607) 255 - 9166

Abstract

Complement is a central part of innate immunity which plays a significant role in the inflammatory response, and many other disease processes. In this study, we analyzed an ensemble of experimentally validated reduced order complement models. Our reduced order modeling approach combined ODEs with logical rules to produce a predictive model with a limited number of equations and parameters. We used this framework to capture the dynamics of C3a and C5a formation in the lectin and alternative pathways. The reduced order model consisted of only 18 differential equations with 28 parameters. Thus, the model was an order of magnitude smaller and included more pathways than comparable ODE models in the literature. We estimated an ensemble of model parameters from *in vitro* time series measurements of the C3a and C5a complement proteins. Subsequently, we validated the model on unseen C3a and C5a measurements that were not used for model training. Given its small size, the hybrid approach produced a surprisingly predictive human complement model. After validation, we performed global sensitivity and robustness analysis to estimate which parameters and species were critical to model performance. These analyses suggested complement was robust to any single therapeutic intervention. The only reliable intervention that consistently reduced C5a formation for all cases was a dual-knockdown of both C3 and C5.

Keywords: Biochemical engineering, systems biology, reduced order models, complement system

1 Introduction

2 Complement is a central part of innate immunity which plays a significant role in the in-
3 flammatory response. Complement was discovered in the 1890s where it was found to
4 'complement' the bactericidal activity of natural antibodies [1]. However, research over
5 the past decade has shown the importance of complement extends well beyond innate
6 immunity. For example, complement contributes to tissue homeostasis by inducing growth
7 factors involved in tissue repair [2]. Complement malfunctions have been linked with sev-
8 eral diseases including Alzheimers, glaucoma, Parkinson's disease, multiple sclerosis,
9 schizophrenia, rheumatoid arthritis and sepsis [3, 4]. Complement can also play both a
10 positive and negative role in certain cancers; attacking tumor cells with altered surface
11 proteins in some cases, while potentially contributing to tumor growth in others [1, 5].
12 Several other important biochemical networks are integrated with complement including
13 the coagulation cascade, the autonomous nervous system and the ability to regulate in-
14 flammation [5]. Thus, complement is an important system involved in a variety of both
15 beneficial and potentially harmful functions in the body.

16 Complement is mediated by over 30 soluble and cell surface proteins that are present
17 as inactive forms in the circulation [6]. The central output of complement activation is the
18 formation of the Membrane Attack Complex (MAC) and a key protein called C5a. The
19 membrane attack complex forms transmembrane channels which disrupt the cell mem-
20 brane of targeted cells, leading to cell lysis and death. The C5a protein acts as a bridge
21 between innate and adaptive immunity, and plays an important role in regulating inflam-
22 mation and coagulation [1]. Complement activation takes places through three pathways:
23 the alternate, the classical and the lectin binding pathway. Each of these pathways in-
24 volves a different initiator signal which leads to a cascade of downstream events in the
25 complement system. The classical pathway is triggered when antibodies form complexes
26 with foreign antigens or other pathogens. A multimeric protein complex C1 binds to the

27 antigen-antibody complex and undergoes a conformational change. This activated com-
28 plex then cleaves complement proteins C4 and C2 into C4a, C4b, C2a and C2b respec-
29 tively. The C4a and C2b fragments combine to form the C4bC2a protease, also known as
30 the classical C3 convertase. The lectin binding pathway is initiated through the binding of
31 L-ficolin or Mannose Binding Lectin (MBL) to carbohydrates on the surfaces of bacterial
32 pathogens. This bound complex in turn cleaves C4 and C2, leading to the formation of
33 C4bC2a. The alternate pathway involves a 'tickover' mechanism in which complement
34 protein C3 is hydrolyzed to form C3b. In the presence of pathogens, the C3b fragment
35 binds foreign surfaces and recruits the additional proteins, factor B and factor D, which
36 lead to the formation of C3bBb, the alternate C3 convertase [7]. The formation of clas-
37 sical and alternate C3 convertases on bacterial surfaces is followed by the formation of
38 proteases called C5 convertases. The classical and alternate C3 convertases recruit C3,
39 Factor B and Factor D to form the classical C5 convertase (C4bC2aC3b), and alternate
40 C5 convertase (C3bBbc3B) respectively. The C5 convertases then cleave C5 to form the
41 C5a and C5b fragments. The cleavage of C5 is followed by a series of sequential cleav-
42 age steps involving the C6, C7, C8 and C9 complement proteins which combine with C5b
43 to form the membrane attack complex [2].

44 Complement activation is regulated by many plasma and host cell proteins. The initi-
45 ation of the classical pathway via complement protein C1 is controlled by the C1 Inhibitor
46 (C1-Inh), a protease inhibitor belonging to the serpin superfamily. C1-Inh irreversibly binds
47 to and deactivates the active subunits of C1, preventing spontaneous fluid phase and
48 chronic activation of complement [8]. Regulation of the upstream elements of comple-
49 ment is also achieved through the interaction of the C4 binding protein (C4BP) with C4b,
50 as well as through the interaction of factor H with C3b [9]. These regulatory proteins
51 are also capable of binding their respective targets while they are bound in convertase
52 complexes. Membrane cofactor protein (MCP or CD46) possesses a cofactor activity for

53 C4b and C3b, which protects the host from self-activation of complement [10]. Delay
54 accelerating factor (DAF or CD55) is also able to recognize and dissociate both C3 and
55 C5 convertases [11]. Carboxypeptidase-N, a well known inflammation regulator, cleaves
56 carboxyl-terminal arginines and lysines of the complement proteins C3a, C4a, and C5a
57 rendering them inactive [12]. Lastly, the assembly of the MAC complex is inhibited by
58 vitronectin and clusterin in the plasma, and CD59 at the host surface [13, 14]. Thus,
59 there are many points of control which influence complement activation across the three
60 activation pathways.

61 Developing quantitative mathematical models of complement could be crucial to un-
62 derstanding its role in the body. Traditionally, complement models have been formulated
63 as systems of linear or non-linear ordinary differential equations (ODEs). For example,
64 Hirayama et al. modeled the classical complement pathway as a system of linear ODEs
65 [15], while Korotaevskiy and co-workers modeled the classical, lectin and alternate path-
66 ways as a system of non-linear ODEs [16]. More recently, large mechanistic models of
67 sections of complement have also been proposed. For example, Liu et al. analyzed the
68 formation of the classical and lectin C3 convertases, and the regulatory role of C4BP
69 using a system of 45 non-linear ODEs with 85 parameters [17]. Recently, Zewde and co-
70 workers constructed a detailed mechanistic model of the alternative pathway which con-
71 sisted of 107 ODEs and 74 kinetic parameters and delineated the complement response
72 of the host and pathogen [14]. However, these previous modeling studies involved little
73 experimental validation. Thus, while these models are undoubtably important theoretical
74 tools, it is unclear if they can describe or quantitatively predict experimentally validated
75 complement dynamics. The central challenge is the estimation of model parameters from
76 experimental data. Unlike other important cascades, such as coagulation for which there
77 are well developed experimental tools and many publicly available data sets, the data for
78 complement is relatively sparse. Missing or incomplete data sets, and limited quantitative

79 data make the identification of mechanistic complement models difficult.

80 In this study, we analyzed an ensemble of reduced order complement models. Our
81 reduced order modeling approach combined ODEs with logical rules to produce a predic-
82 tive model with a limited number of equations and parameters. We used this framework
83 to capture the dynamics of C3a and C5a formation in the lectin and alternative pathways.
84 The reduced order model consisted of 18 differential equations with 28 parameters. The
85 model was an order of magnitude smaller and included more pathways than compara-
86 ble ODE models in the literature. We estimated an ensemble of model parameters from
87 *in vitro* time series measurements of C3a and C5a from Morad and coworkers [18]. Sub-
88 sequently, we validated the model by predicting C3a and C5a measurements that were not
89 used for model training. Given its small size, the hybrid approach produced a surprisingly
90 predictive human complement model. After validation, we performed a global analysis
91 on the model ensemble to estimate which parameters were critical to model performance
92 under different experimental conditions and to identify potential therapeutic targets.

93 **Results**

94 **Reduced order complement network.** The reduced order complement model described
95 the alternate and lectin pathways (Fig. 1). A trigger event initiated the lectin pathway,
96 which activated the cleavage of C2 and C4 into C2a, C2b, C4a and C4b respectively.
97 Classical Pathway (CP) C3 convertase (C4aC2b) then catalyzed the cleavage of C3 into
98 C3a and C3b. Activation of the alternative pathway was initiated through the spontaneous
99 hydrolysis of C3 into C3a and C3b. The C3b fragment then recombined with C3 to form
100 the alternate pathway (AP) C3 convertase. Both the CP and AP C3 convertases catalyzed
101 the cleavage of C3 into C3a and C3b. A second C3b fragment could then bind with either
102 the CP or AP C3 convertase to form the CP (or AP) C5 convertase. The C5 convertase
103 catalyzed the cleavage of C5 into the C5a and C5b fragments. Lectin pathway activation
104 was approximated using a combination of saturation kinetics and non-linear transfer func-
105 tions, which facilitated a significant reduction in the size of the model while maintaining
106 performance. Thus, while the reduced order complement model encoded significant bio-
107 logical complexity, it was highly compact consisting of only 18 differential equations and
108 28 model parameters. Next, we estimated an ensemble of model parameters from time
109 series measurements of the C3a and C5a complement proteins.

110 **Estimating an ensemble of reduced order complement models.** A critical challenge
111 for any dynamic model is the estimation of model parameters. We estimated the com-
112 plement model parameters in a hierarchical fashion using two *in vitro* time-series data
113 sets generated with and without zymosan, a lectin pathway activator [18]. The residual
114 between model simulations and experimental measurements was minimized using the dy-
115 namic optimization with particle swarms (DOPS) approach, starting from an initial random
116 parameter guess. A hierarchical approach was taken to determine model parameters in
117 which the alternate pathway parameters were first estimated and then fixed during the
118 estimation of the lectin pathway parameters. The reduced order complement model cap-

tured the behavior of the alternative and lectin pathways (Fig. 2). For the alternative pathway, we used the C3a and C5a measurements in the absence of zymosan, and only allowed the alternative parameters to vary (Fig. 2A and B). Lectin parameters were estimated from C3a and C5a measurements in the presence of 1g zymosan (Fig. 2C and D). Taken together, the reduced order model reproduced a panel of lectin pathway initiation data sets in the neighborhood of physiological factor and inhibitor concentrations. However, it was unclear whether the reduced order model could predict new data, without updating the model parameters. To address this question, we fixed the model parameters and simulated data not used for model training.

We tested the predictive power of the reduced order complement model with data not used during model training (Fig. 3). Six validation cases were considered, three for C3a and C5a respectively at different zymosan concentrations. All model parameters were fixed for the validation simulations. The ensemble of reduced order models captured the qualitative dynamics of C3a formation (Fig. 3, left column), and C5a formation (Fig. 3, right column) at three inducer concentrations. However, there were shortcomings, especially for the C3a prediction. First, while the C3a dynamics and concentration peak times were captured, the overall level of C3a was under-predicted in all cases (Fig. 3, inset left column). We believe the C3a under-prediction can be attributed to how we modeled C4BP interactions. C4BP interactions were modeled as irreversible binding steps resulting in completely inactive complexes; however, the binding of C4BP with complement proteins is likely reversible and convertases may have residual activity even in the bound form. Thus, the model may over-predict the influence of C4BP. We also failed to capture the concave down curvature for the 0.001 g and 0.01 g zymosan cases in the C5a validation studies. The decreasing slope of the C5a measurements may indicate decreasing cofactors abundance, or missing biology which we have not explicitly accounted for in the reduced order approach. However, despite these shortcomings, we qualitatively pre-

145 dicted unseen experimental data, including correctly capturing the dynamic time scale of
146 C3a formation, and the correct order of magnitude for the concentration of C5a for three
147 inducer levels. Next, we used global sensitivity and robustness analysis to determine
148 which parameters and species controlled the performance of the complement model.

149 **Global analysis of the reduced order complement model** We conducted sensitivity
150 analysis to estimate which parameters controlled the performance of the reduced order
151 complement model. We calculated the sensitivity of the C3a and C5a residuals with and
152 without zymosan for the ensemble of parameter sets (Fig. 4A - D). In the absence of zy-
153 mosan (where only the alternative pathway is active), $k_{f,C3b}$ (formation of C3b) and $k_{d,C3a}$
154 (degradation rate constant governing C3a) were largely responsible for the system re-
155 sponse. Interestingly, $k_{c,C3}$ (the rate constant governing AP C3-convertase activity) was
156 not sensitive in the absence of zymosan. Thus, the behavior of the alternative pathway
157 was more heavily influenced by the spontaneous hydrolysis of C3, rather than AP C3-
158 convertase activity. On the other hand, $k_{c,C3}$ was one of the parameters that controlled
159 C5a formation, in addition to the expected parameters related to AP C5-convertase for-
160 mation. The AP C3-convertase is required for AP C5-convertase formation, and the for-
161 mation of the C3b fragment. Thus, changes in the activity of AP C3-convertase will not
162 drastically change the C3a dynamics, but will effect AP C5-convertase activity and C5a
163 formation. The sensitivity analysis yielded the expected results for the lectin pathway that
164 included parameters sensitive to pathway initiation (Fig. 4C and D). One key difference
165 observed between the sensitivity of C3a and C5a parameters, was their respective degra-
166 dation constants. The rate constant governing C3a degradation was sensitive, while the
167 degradation constant for C5a was not. This difference was likely attributable to the mag-
168 nitude of the degradation parameters and the respective concentrations of C3a and C5a.
169 Thus, sensitivity analysis identified important indirect parameter interactions that could
170 have therapeutic significance. However, sensitivity coefficients are a local measure of

171 how small changes in a parameter value effects a performance objective, for example the
172 abundance of C5a. To more closely simulate a clinical intervention e.g., administration of
173 an anti-complement antibody, we performed robustness analysis. Robustness coefficients
174 quantify the response of a marker to a macroscopic structural or operational perturbation
175 to the network architecture. In this case, we computed how the C3a and C5a trajectories
176 responded to a decrease in the initial abundance of C3 and C5.

177 Robustness analysis suggested there was no single intervention that inhibited com-
178 plement activation in the presence of both initiation pathways (Fig. 5). We calculated
179 robustness indices for C3a and C5a for the 50 parameter sets in the ensemble with and
180 without the lectin pathway initiator. We simulated the addition of different doses of anti-
181 complement antibody cocktails by decreasing the initial concentration of C3 or C5 or the
182 combination of C3 and C5 by 50% and 90%. A \log_{10} transformed robustness index of
183 zero indicated no effect due to the perturbation, whereas an index of less than zero in-
184 dicated decreased C3a or C5a. As expected, a C5 knockdown had no effect on C3a
185 formation for either the alternate (Fig. 5A, lanes 1 or 3) or lectin pathways (Fig. 5B, lanes
186 1 or 3). However, C3a abundance and to a lesser extent C5a abundance decreased with
187 decreasing C3 concentration in the alternate pathway (Fig. 5A or B, lanes 1 or 2). This
188 agreed with the sensitivity results; changes in AP C3-convertase formation or activity af-
189 fected the downstream dynamics of C5a formation. Thus, these results suggested that C3
190 alone would be a reasonable target, especially given that C5a formation was surprisingly
191 robust to C5 levels in the alternate pathway (Fig. 5A or B, lane 2). Yet, in lectin initiated
192 complement activation, C5a levels were robust to the initial C3 concentration (Fig. 5A or
193 B, lane 4). Thus, above some limiting threshold, even small concentrations of C3 and C5
194 convertases catalyzed the downstream formation of C5a. The only reliable intervention
195 that consistently reduced C5a formation for all cases was a dual-knockdown. For exam-
196 ple, a 90% decrease of both C3 and C5 reduced the formation of C5a by over an order of

¹⁹⁷ magnitude (Fig. 5B, lane 4).

198 **Discussion**

199 In this study, we analyzed an ensemble of reduced order complement models. The re-
200 duced order modeling approach combined ODEs with logical rules to produce a predictive
201 model with a limited number of equations and parameters. The reduced order model con-
202 sisted of only 18 differential equations with 28 parameters. Thus, the model was an order
203 of magnitude smaller and included more pathways than comparable ODE models in the
204 literature. We used this framework to simulate the dynamics of C3a and C5a formation
205 in the lectin and alternative pathways. We estimated an ensemble of model parame-
206 ters from *in vitro* time series measurements of C3a and C5a abundance. Subsequently,
207 we validated the model on unseen C3a and C5a measurements that were not used for
208 model training. Given its small size, the hybrid approach produced a surprisingly predic-
209 tive complement model. After validation, we performed a global sensitivity analysis on the
210 model ensemble to estimate which parameters were critical to model performance under
211 different experimental conditions. The global sensitivity analysis identified important indi-
212 rect parameter interactions that could have therapeutic significance including convertase
213 formation and activity as well as C3 and C5 inhibition. Subsequently we performed a
214 robustness analysis where we analyzed the effect of perturbing initial C3 and C5 levels
215 on the total amount of C3a and C5a generated. Using a simple and versatile modeling
216 approach, we developed a reduced order complement model that is computationally inex-
217 pensive, and one that could easily be incorporated into pre-existing or new pharmacoki-
218 netic models. Furthermore this approach model has the potential to create individualized
219 treatment plans for patients with complement deficiency.

220 Despite its importance, there has been a paucity of validated mathematical models
221 of complement pathway activation. To our knowledge, this study is one of the first com-
222 plement models that combined multiple initiation pathways with experimental validation
223 of important complement products like C5a. However, there have been several theoreti-

224 cal models of components of the cascade in the literature. Liu and co-workers modeled
225 the formation of C3a through the classical pathway using 45 non-linear ODEs [17]. In
226 contrast, in this study we modeled lectin mediated C3a formation using only five ODEs.
227 Though we did not model all the initiation interactions in detail, especially the cross-talk
228 between the lectin and classical pathways, we successfully captured C3a dynamics with
229 respect to different concentrations of lectin initiators. The model also captured the dy-
230 namics of C3a and C5a formed from the alternate pathway using only seven ODEs. The
231 reduced order model predictions of C5a were qualitatively similar to the theoretical com-
232 plement model of Zewde et al which involved over 100 ODEs [14]. However, we found
233 that the quantity of C3a produced in the alternate pathway was nearly 1000 times the
234 quantity of C5a produced. Though this was in agreement with the experimental data [18],
235 it differed from the theoretical predictions made by Zewde et al. who showed C3a was 10^8
236 times the C5a concentration [14]. In our model, the time profile of C5a generation from the
237 lectin pathway changed with respect to the quantity of zymosan (the lectin pathway initia-
238 tor). The lag phase for generation was inversely proportional to the initiator concentration.
239 Korotaevskiy et al. showed a similar trend using a theoretical model of complement, albeit
240 for much shorter time scales [16]. Thus, the reduced order complement model performed
241 similarly to existing large mechanistic models, despite being significantly smaller.

242 Global analysis of the complement model estimated potential important therapeutic
243 targets. Complement malfunctions are implicated in a number of diseases, however the
244 development of complement specific therapeutics has been challenging [3, 19]. Previ-
245 ously, we have shown that mathematical modeling and sensitivity analysis can be useful
246 tools to estimate therapeutically important mechanisms in biochemical networks [20–23].
247 In this study, we analyzed a validated ensemble of reduced order complement models to
248 estimate therapeutically important mechanisms. In presence of an initiator, C5a forma-
249 tion was primarily sensitive to the lectin initiation parameters, and parameters governing

250 the conversion of C5 to C5a and C5b. This result agrees well with the current protease
251 inhibitors targeting initiating complexes, including mannose-associated serine proteases
252 1 and 2 (MASP-1,2) [24]. The most commonly used anti-complement drug eculizumab
253 [19], targets the C5 protein which is cleaved to form C5a. Our sensitivity analysis showed
254 that kinetic parameters governing C5 conversion were sensitive in both lectin initiated and
255 alternate pathways, thus agreeing with targeting C5 protein. The formation of basal C3b
256 was also a sensitive parameter in the formation of C3a through the alternate pathway.
257 Thus, this mechanism can act as a target for both C3a and C5a inhibitors. Lectin initiated
258 C3a formation showed a number of sensitive parameters. This included the lectin initi-
259 ation parameters that controlled C5a formation, C3 convertase inhibition by C4BP, and
260 parameters governing C3 convertase activity. All these mechanisms are potential drug
261 targets.

262 To further validate these results from sensitivity analysis about potential drug targets
263 we did a robustness analysis. We knocked down C3 and C5 levels and studied their im-
264 pact on the generation of C3a and C5a. The C3a and C5a levels in the lectin pathway
265 were strongly influenced by initial levels of C3 and C5. Thus direct inhibition of C3 and
266 C5, or targeting complexes (MASP complex, C3 and C5 convertases) that act on C3 and
267 C5 have a direct impact on production of C3a and C5a. This is also in agreement with
268 sensitivity analysis that C5 is a good drug target. A number of drugs targeting C5 are
269 being developed. For example LFG316 by Novartis is being used to target C5 in cases
270 of Age-Related Macular Degeneration [25], Mubodina is an antibody that targets C5 in
271 the treatment of Atypical Hemolytic-Uremic Syndrome (aHUS) [26], Coversin is a small
272 molecule targeting C5 [27], Zimura is an aptamer targeting C5 [28], small peptides and
273 RNAi are also being used to inhibit C5 [29]. Another important conclusion that can be
274 drawn together from sensitivity and robustness analysis is that C3 and C5 convertases
275 can be important therapeutic targets. Though knockdown of C3 and C5 affects C3a and

276 C5a levels downstream, the abundance and turnover rate [30, 31] of these proteins make
277 them difficult targets. Thus targeting C3 and C5 directly will require high dosage of drugs.
278 It is also well known that eculizumab dosage needs to be adjusted while treating for Atyp-
279 ical Hemolytic-Uremic Syndrome (aHUS), a disease that is caused due to uncontrolled
280 complement activation [32]. The issue of high dosage can potentially be circumvented
281 by targeting convertases or fragile mechanisms that involve C3, C5 or their activated
282 components. Our analysis shows that formation and assembly of these convertases are
283 sensitive mechanisms that strongly impact downstream proteins like C5a. Formation of
284 convertases is inhibited by targeting upstream protease complexes like MASP-1,2 from
285 lectin pathway (or C1r, C1s from classical pathway). For example, Omeros is a protease
286 inhibitor that targets MASP-2 complex and thereby inhibits formation of downstream con-
287 vertases [33]. Lampalizumab (an immunoglobulin) and Bikaciomab (an antibody frag-
288 ment) target Factor B and Factor D respectively. Factor B and Factor D are crucial to
289 formation alternate pathway convertases [34, 35]. Novelmed Therapeutics recently de-
290 veloped antibody, NM9401 against propedin, a small protein that stabilizes alternate C3
291 convertase [36]. Cobra Venom Factor (CVF), an analogue of C3b has been used to bind
292 to Factor B to regulate alternate convertases [37]. Thus, analysis of the ensemble of com-
293 plement models identified potentially important therapeutic targets that are consistent with
294 therapeutic strategies that are under development.

295 The performance of the complement model was impressive given its limited size. How-
296 ever, there are several questions that should be explored further. A logical progression for
297 this work would be to expand the network to include the classical pathway and the forma-
298 tion of the membrane attack complex (MAC). However, it is unclear whether the addition
299 of the classical pathway will decrease the predictive quality of our existing model. Liu
300 et al have shown cross-talk between the activation of the classical and lectin pathways
301 that could influence model performance [17]. One potential approach to address such

302 difficulties would be to incorporate C reactive proteins (CRP) and L-ficolin (LF) into the
303 model, both of which are involved with the initiation of classical and lectin pathways. Liu
304 et al. showed that under inflammation conditions interactions between lectin and classical
305 pathways was mediated through CRP and LF [17]. Thus incorporating these two proteins
306 would help us in modeling cross talk. Time course measurements of MAC abundance
307 (and MAC formation dynamics) are also scarce, making the inclusion of MAC challeng-
308 ing. Next, we should address the under-prediction of C3a. We believe the C3a under-
309 prediction can be attributed to how we modeled C4BP interactions. C4BP interactions
310 were modeled as irreversible binding steps resulting in completely inactive complexes;
311 however, the binding of C4BP with complement proteins is likely reversible and C4BP-
312 bound convertases may have residual activity. We also did not capture the maximum
313 concentration of C3a at low initiator levels. One possible reasons for this could be the C2-by
314 pass pathway, which was not included in the model. This pathway further accelerates C3a
315 production without the involvement of a C3 convertase. Currently the C3a in the model is
316 generated only through the activity of a C3 convertase. Incorporating this additional step
317 within the reduced order modeling framework would be a future direction that we need
318 to consider. We should test alternative model structures which include reversible C4BP
319 binding, and partially active convertases. Alternatively, we could also perform sensitivity
320 analysis on the C3a prediction residual to determine which parameters controlled the C3a
321 prediction.

322 **Materials and Methods**

323 We used ordinary differential equations (ODEs) to model the time evolution of complement
 324 proteins (x_i) in the reduced order model:

$$\frac{dx_i}{dt} = \sum_{j=1}^{\mathcal{R}} \sigma_{ij} r_j(\mathbf{x}, \epsilon, \mathbf{k}) \quad i = 1, 2, \dots, \mathcal{M} \quad (1)$$

325 where \mathcal{R} denotes the number of reactions and \mathcal{M} denotes the number of protein species
 326 in the model. The quantity $r_j(\mathbf{x}, \epsilon, \mathbf{k})$ denotes the rate of reaction j . Typically, reaction j is
 327 a non-linear function of biochemical and enzyme species abundance, as well as unknown
 328 model parameters \mathbf{k} ($\mathcal{K} \times 1$). The quantity σ_{ij} denotes the stoichiometric coefficient for
 329 species i in reaction j . If $\sigma_{ij} > 0$, species i is produced by reaction j . Conversely, if $\sigma_{ij} < 0$,
 330 species i is consumed by reaction j , while $\sigma_{ij} = 0$ indicates species i is not connected
 331 with reaction j . Species balances were subject to the initial conditions $\mathbf{x}(t_0) = \mathbf{x}_0$.

332 Rate processes were written as the product of a kinetic term (\bar{r}_j) and a control term
 333 (v_j) in the complement model. The kinetic term for the formation of C4a, C4b, C2a and
 334 C2b, lectin pathway activation, and C3 and C5 convertase activity was given by:

$$\bar{r}_j = k_j^{max} \epsilon_i \left(\frac{x_s^\eta}{K_{js}^\eta + x_s^\eta} \right) \quad (2)$$

335 where k_j^{max} denotes the maximum rate for reaction j , ϵ_i denotes the abundance of the
 336 enzyme catalyzing reaction j , η denotes a cooperativity parameter, and K_{js} denotes the
 337 saturation constant for species s in reaction j . We used mass action kinetics to model
 338 protein-protein binding interactions within the network:

$$\bar{r}_j = k_j^{max} \prod_{s \in m_j^-} x_s^{-\sigma_{sj}} \quad (3)$$

339 where k_j^{max} denotes the maximum rate for reaction j , σ_{sj} denotes the stoichiometric coefficient
 340 for species s in reaction j , and $s \in m_j$ denotes the set of *reactants* for reaction j .
 341 The control terms $0 \leq v_j \leq 1$ depended upon the combination of factors which influenced
 342 rate process j . For each rate, we used a rule-based approach to select from competing
 343 control factors. If rate j was influenced by $1, \dots, m$ factors, we modeled this relationship
 344 as $v_j = \mathcal{I}_j(f_{1j}(\cdot), \dots, f_{mj}(\cdot))$ where $0 \leq f_{ij}(\cdot) \leq 1$ denotes a regulatory transfer function
 345 quantifying the influence of factor i on rate j . The function $\mathcal{I}_j(\cdot)$ is an integration rule which
 346 maps the output of regulatory transfer functions into a control variable. Each regulatory
 347 transfer function took the form:

$$f_{ij}(\mathcal{Z}_i, k_{ij}, \eta_{ij}) = k_{ij}^{\eta_{ij}} \mathcal{Z}_i^{\eta_{ij}} / (1 + k_{ij}^{\eta_{ij}} \mathcal{Z}_i^{\eta_{ij}}) \quad (4)$$

348 where \mathcal{Z}_i denotes the abundance of factor i , k_{ij} denotes a gain parameter, and η_{ij} denotes
 349 a cooperativity parameter. In this study, we used $\mathcal{I}_j \in \{min, max\}$ [38]. If a process has
 350 no modifying factors, $v_j = 1$. The model equations were implemented in MATLAB and
 351 solved using the ODE23s routine (The Mathworks, Natick MA). The complement model
 352 code and parameter ensemble is freely available under an MIT software license and can
 353 be downloaded from <http://www.varnerlab.org>.

354 **Estimation of an ensemble of model parameters.** We minimized the residual between
 355 simulations and experimental C3a and C5a measurements using Dynamic Optimization
 356 with Particle Swarms (DOPS). DOPS minimized the objective:

$$\min_{\mathbf{k}} \sum_{\tau=1}^{\mathcal{T}} \sum_{j=1}^{\mathcal{S}} \left(\frac{\hat{x}_j(\tau) - x_j(\tau, \mathbf{k})}{\omega_j(\tau)} \right)^2 \quad (5)$$

357 where $\hat{x}_j(\tau)$ denotes the measured value of species j at time τ , $x_j(\tau, \mathbf{k})$ denotes the simulated
 358 value for species j at time τ , and $\omega_j(\tau)$ denotes the experimental measurement

variance for species j at time τ . The outer summation is with respect to time, while the inner summation is with respect to state. DOPS is a novel metaheuristic that combines multi swarm particle swarm optimization (PSO) with a greedy global optimization algorithm called dynamically dimensioned search (DDS). DOPS is faster than conventional global optimizers and has the ability to find near optimal solutions for high dimensional systems within a relatively few function evaluations. It uses an adaptive switching strategy based on error convergence rates to switch from the particle swarm to DDS search phases. This enables DOPS to quickly estimate globally optimal or near optimal solutions even in the presence of many local minima. In the swarm search, for each iteration the particles compute error within each sub-swarm by evaluating the model equations using their specific parameter vector realization. From each of these points within a sub-swarm a local best is identified. This along with the particle best within the sub-swarm \mathcal{S}_k is used to update the parameter estimate for each particle using the following rules:

$$z_{i,j} = \theta_1 z_{i,j-1} + \theta_2 r_1 (\mathcal{L}_i - z_{i,j-1}) + \theta_3 r_2 (\mathcal{G}_k - z_{i,j-1}) \quad (6)$$

where $z_{i,j}$ is the parameter vector, $(\theta_1, \theta_2, \theta_3)$ were adjustable parameters, \mathcal{L}_i denotes the best solution found by particle i within sub-swarm \mathcal{S}_k for function evaluations $1 \rightarrow j-1$, and \mathcal{G}_k denotes the best solution found over all particles within sub-swarm \mathcal{S}_k . The quantities r_1 and r_2 denote uniform random vectors with the same dimension as the number of unknown model parameters ($\mathcal{K} \times 1$). At the conclusion of the swarm phase, the overall best particle, \mathcal{G}_k , over the k sub-swarms was used to initialize the DDS phase. For the DDS phase, the best parameter estimate was updated using the rule:

$$\mathcal{G}_{new}(J) = \begin{cases} \mathcal{G}(J) + \mathbf{r}_{normal}(J)\sigma(J), & \text{if } \mathcal{G}_{new}(J) < \mathcal{G}(J). \\ \mathcal{G}(J), & \text{otherwise.} \end{cases} \quad (7)$$

379 where \mathbf{J} is a vector representing the subset of dimensions that are being perturbed, \mathbf{r}_{normal}
380 denotes a normal random vector of the same dimensions as \mathcal{G} , and σ denotes the pertur-
381 bation amplitude:

$$\sigma = R(\mathbf{p}^U - \mathbf{p}^L) \quad (8)$$

382 where R is the scalar perturbation size parameter, \mathbf{p}^U and \mathbf{p}^L are $(\mathcal{K} \times 1)$ vectors that
383 represent the maximum and minimum bounds on each dimension. The set \mathbf{J} was con-
384 structed using a monotonically decreasing probability function \mathcal{P}_i that represents a thresh-
385 old for determining whether a specific dimension j was perturbed or not. DDS updates
386 are greedy; \mathcal{G}_{new} becomes the new solution vector only if it is better than \mathcal{G} . At the end of
387 DDS phase we obtain the optimal vector \mathcal{G} which we use for plotting best fits against the
388 experimental data, and for generating a parameter ensemble.

389 An ensemble of parameters was obtained by randomly perturbing the optimal param-
390 eter set within bounds established by perturbing each parameter and measuring the in-
391 crease in the residual. Thereafter, the optimal parameter vector was perturbed within
392 these bounds for approximately 100,000 iterations. Within each iteration the quality of
393 perturbed vector was measured using goodness of fit (model residual). If the residual was
394 too high or the perturbed vector generated a numerical error, the vector was rejected. We
395 selected an ensemble of $N = 50$ parameter sets for this study using this sampling proce-
396 dure. The DOPS routine was implemented in MATLAB (The Mathworks, Natick MA) and
397 can be downloaded from <http://www.varnerlab.org>.

398 **Sensitivity and robustness analysis of model performance.** We conducted global
399 sensitivity and robustness analysis to estimate which parameters and species controlled
400 the performance of the reduced order model. We computed the total variance-based sen-
401 sitivity index of each parameter relative to the training residual for the C3a alternate, C5a
402 alternate, C3a lectin, and C5a lectin cases using the Sobol method [39]. The sampling

403 bounds for each parameter were established from the minimum and maximum value for
 404 that parameter in the parameter ensemble. We used the sampling method of Saltelli *et*
 405 *al.* to compute a family of $N(2d + 2)$ parameter sets which obeyed our parameter ranges,
 406 where N was the number of trials per parameters, and d was the number of parameters
 407 in the model [40]. In our case, $N = 200$ and $d = 28$, so the total sensitivity indices were
 408 computed using 11,600 model evaluations. The variance-based sensitivity analysis was
 409 conducted using the SALib module encoded in the Python programming language [41].

410 Robustness coefficients quantify the response of a marker to a structural or opera-
 411 tional perturbation to the network architecture. Robustness coefficients were calculated
 412 as shown previously [42]. Robustness coefficients denoted by $\alpha(i, j, t_o, t_f)$ are defined
 413 as:

$$\alpha(i, j, t_o, t_f) = \log_{10} \left[\left(\int_{t_o}^{t_f} x_i(t) dt \right)^{-1} \left(\int_{t_o}^{t_f} x_i^{(j)}(t) dt \right) \right] \quad (9)$$

414 Here t_o and t_f denote the initial and final simulation time respectively, while i and j denote
 415 the indices for the marker and the perturbation respectively. A value of $\alpha(i, j, t_o, t_f) >$
 416 0, indicates increased marker abundance, while $\alpha(i, j, t_o, t_f) < 0$ indicates decreased
 417 marker abundance following perturbation j . If $\alpha(i, j, t_o, t_f) \sim 0$ the j th perturbation did not
 418 influence the abundance of marker i . In this study, we perturbed the initial condition of C3
 419 or C5 or a combination of C3 and C5 by 50% or 90% and measured the area under the
 420 curve (AUC) of C3a or C5a with and without lectin initiator. Robustness coefficients were
 421 calculated for every member of the ensemble, where the mean $\pm 1 \times$ standard-deviation
 422 are reported.

423 **Competing interests**

424 The authors declare that they have no competing interests.

425 **Author's contributions**

426 J.V directed the study. A.S developed the reduced order complement model and the
427 parameter ensemble. W.D and M.M analyzed model simulations and generated figures
428 for the manuscript. The manuscript was prepared and edited for publication by A.S, W.D,
429 M.M and J.V.

430 **Acknowledgements**

431 We gratefully acknowledge the suggestions from the anonymous reviewers to improve
432 this manuscript.

433 **Funding**

434 This study was supported by an award from the US Army and Systems Biology of Trauma
435 Induced Coagulopathy (W911NF-10-1-0376) to J.V. for the support of A.S.

436 **References**

- 437 1. Sarma JV, Ward PA (2011) The complement system. *Cell and tissue research* 343:
438 227–235.
- 439 2. Ricklin D, Hajishengallis G, Yang K, Lambris JD (2010) Complement: a key system
440 for immune surveillance and homeostasis. *Nature immunology* 11: 785–797.
- 441 3. Ricklin D, Lambris JD (2007) Complement-targeted therapeutics. *Nature biotechnol-*
442 *ogy* 25: 1265-1275.
- 443 4. Rittirsch D, Flierl MA, Ward PA (2008) Harmful molecular mechanisms in sepsis. *Na-*
444 *ture Reviews Immunology* 8: 776–787.
- 445 5. Ricklin D, Lambris JD (2013) Complement in immune and inflammatory disorders:
446 pathophysiological mechanisms. *The Journal of Immunology* 190: 3831–3838.
- 447 6. Walport MJ (2001) Complement. first of two parts. *The New England journal of*
448 *medicine* 344: 1058–1066.
- 449 7. Pangburn MK, Müller-Eberhard HJ (1984) The alternative pathway of complement.
450 Springer seminars in immunopathology .
- 451 8. Walker D, Yasuhara O, Patston P, McGeer E, McGeer P (1995) Complement c1 in-
452 hibitor is produced by brain tissue and is cleaved in alzheimer disease. *Brain research*
453 675: 75–82.
- 454 9. Blom AM, Kask L, Dahlbäck B (2001) Structural requirements for the complement
455 regulatory activities of c4bp. *Journal of Biological Chemistry* 276: 27136–27144.
- 456 10. Riley-Vargas RC, Gill DB, Kemper C, Liszewski MK, Atkinson JP (2004) Cd46: ex-
457 panding beyond complement regulation. *Trends in immunology* 25: 496–503.
- 458 11. Lukacik P, Roversi P, White J, Esser D, Smith G, et al. (2004) Complement regulation
459 at the molecular level: the structure of decay-accelerating factor. *Proceedings of the*
460 *National Academy of Sciences of the United States of America* 101: 1279–1284.
- 461 12. Liszewski MK, Farries TC, Lublin DM, Rooney IA, Atkinson JP (1995) Control of the

- 462 complement system. *Advances in immunology* 61: 201–283.
- 463 13. Chauhan A, Moore T (2006) Presence of plasma complement regulatory proteins
464 clusterin (apo j) and vitronectin (s40) on circulating immune complexes (cic). *Clinical
465 & Experimental Immunology* 145: 398–406.
- 466 14. Zewde N, Gorham Jr RD, Dorado A, Morikis D (2016) Quantitative modeling of the
467 alternative pathway of the complement system. *PloS one* 11: e0152337.
- 468 15. Hirayama H, Yoshii K, Ojima H, Kawai N, Gotoh S, et al. (1996) Linear systems analy-
469 sis of activating processes of complement system as a defense mechanism. *Biosys-
470 tems* 39: 173–185.
- 471 16. Korotaevskiy AA, Hanin LG, Khanin MA (2009) Non-linear dynamics of the comple-
472 ment system activation. *Mathematical biosciences* 222: 127–143.
- 473 17. Liu B, Zhang J, Tan PY, Hsu D, Blom AM, et al. (2011) A computational and experi-
474 mental study of the regulatory mechanisms of the complement system. *PLoS Comput
475 Biol* 7: e1001059.
- 476 18. Morad HO, Belete SC, Read T, Shaw AM (2015) Time-course analysis of c3a and
477 c5a quantifies the coupling between the upper and terminal complement pathways in
478 vitro. *Journal of immunological methods* 427: 13–18.
- 479 19. Morgan BP, Harris CL (2015) Complement, a target for therapy in inflammatory and
480 degenerative diseases. *Nature Reviews Drug Discovery* 14: 857-877.
- 481 20. Luan D, Zai M, Varner JD (2007) Computationally derived points of fragility of a human
482 cascade are consistent with current therapeutic strategies. *PLoS Comput Biol* 3:
483 e142.
- 484 21. Nayak S, Salim S, Luan D, Zai M, Varner JD (2008) A test of highly optimized tol-
485 erance reveals fragile cell-cycle mechanisms are molecular targets in clinical cancer
486 trials. *PLoS One* 3: e2016.
- 487 22. Tasseff R, Nayak S, Salim S, Kaushik P, Rizvi N, et al. (2010) Analysis of the molecular

- 488 networks in androgen dependent and independent prostate cancer revealed fragile
489 and robust subsystems. PLoS One 5: e8864.
- 490 23. Rice NT, Szlam F, Varner JD, Bernstein PS, Szlam AD, et al. (2016) Differential con-
491 tributions of intrinsic and extrinsic pathways to thrombin generation in adult, maternal
492 and cord plasma samples. PLoS One 11: e0154127.
- 493 24. Héja D, Harmat V, Fodor K, Wilmanns M, Dobó J, et al. (2012) Monospecific inhibitors
494 show that both mannan-binding lectin-associated serine protease-1 (masp-1) and-2
495 are essential for lectin pathway activation and reveal structural plasticity of masp-2.
496 Journal of Biological Chemistry : 20290–20300.
- 497 25. Roguska M, Splawski I, Diefenbach-Streiber B, Dolan E, Etemad-Gilbertson B, et al.
498 (2014) Generation and characterization of IgG316, a fully-human anti-c5 antibody for
499 the treatment of age-related macular degeneration. Investigative Ophthalmology &
500 Visual Science : 3433–3433.
- 501 26. Melis JP, Strumane K, Ruuls SR, Beurskens FJ, Schuurman J, et al. (2015) Com-
502 plement in therapy and disease: Regulating the complement system with antibody-
503 based therapeutics. Molecular immunology : 117–130.
- 504 27. Weston-Davies WH, Nunn MA, Pinto FO, Mackie IJ, Richards SJ, et al. (2014) Clin-
505 ical and immunological characterisation of coversin, a novel small protein inhibitor of
506 complement c5 with potential as a therapeutic agent in pnh and other complement
507 mediated disorders. Blood : 4280–4280.
- 508 28. Epstein D, Kurz JC (2007). Complement binding aptamers and anti-c5 agents useful
509 in the treatment of ocular disorders. US Patent App. 12/224,708.
- 510 29. Borodovsky A, Yucius K, Sprague A, Banda NK, Holers VM, et al. (2014) Aln-cc5, an
511 investigational rnai therapeutic targeting c5 for complement inhibition. Complement :
512 40.
- 513 30. Sissons J, Liebowitch J, Amos N, Peters D (1977) Metabolism of the fifth component

- 514 of complement, and its relation to metabolism of the third component, in patients with
515 complement activation. *Journal of Clinical Investigation* : 704.
- 516 31. Swaak A, Hannema A, Vogelaar C, Boom F, van Es L, et al. (1982) Determination of
517 the half-life of c3 in patients and its relation to the presence of c3-breakdown products
518 and/or circulating immune complexes. *Rheumatology international* : 161–166.
- 519 32. Noris M, Galbusera M, Gastoldi S, Macor P, Banterla F, et al. (2014) Dynamics of
520 complement activation in ahus and how to monitor eculizumab therapy. *Blood* : 1715–
521 1726.
- 522 33. Schwaebel HW, Stover CM, Tedford CE, Parent JB, Fujita T (2011). Methods for
523 treating conditions associated with masp-2 dependent complement activation. US
524 Patent 7,919,094.
- 525 34. Katschke KJ, Wu P, Ganesan R, Kelley RF, Mathieu MA, et al. (2012) Inhibiting al-
526 ternative pathway complement activation by targeting the factor d exosite. *Journal of*
527 *Biological Chemistry* : 12886–12892.
- 528 35. Hu X, Holers VM, Thurman JM, Schoeb TR, Ramos TN, et al. (2013) Therapeutic
529 inhibition of the alternative complement pathway attenuates chronic eae. *Molecular*
530 *immunology* : 302–308.
- 531 36. Bansal R (2014). Humanized and chimeric anti-properdin antibodies. US Patent
532 8,664,362.
- 533 37. Vogel CW, Fritzinger DC, Hew BE, Thorne M, Bammert H (2004) Recombinant cobra
534 venom factor. *Molecular immunology* : 191–199.
- 535 38. Sagar A, Varner JD (2015) Dynamic modeling of the human coagulation cascade
536 using reduced order effective kinetic models. *Processes* 3: 178.
- 537 39. Sobol I (2001) Global sensitivity indices for nonlinear mathematical models and their
538 monte carlo estimates. *Mathematics and Computers in Simulation* 55: 271 - 280.
- 539 40. Saltelli A, Annoni P, Azzini I, Campolongo F, Ratto M, et al. (2010) Variance based

- 540 sensitivity analysis of model output. design and estimator for the total sensitivity index.
- 541 Computer Physics Communications 181: 259–270.
- 542 41. Herman J. Salib: Sensitivity analysis library in python (numpy). con-
- 543 tains sobol, morris, fractional factorial and fast methods. available online:
- 544 <https://github.com/jdherman/salib>.
- 545 42. Tasseff R, Nayak S, Song SO, Yen A, Varner JD (2011) Modeling and analysis
- 546 of retinoic acid induced differentiation of uncommitted precursor cells. Integr Biol
- 547 (Camb) 3: 578-91.

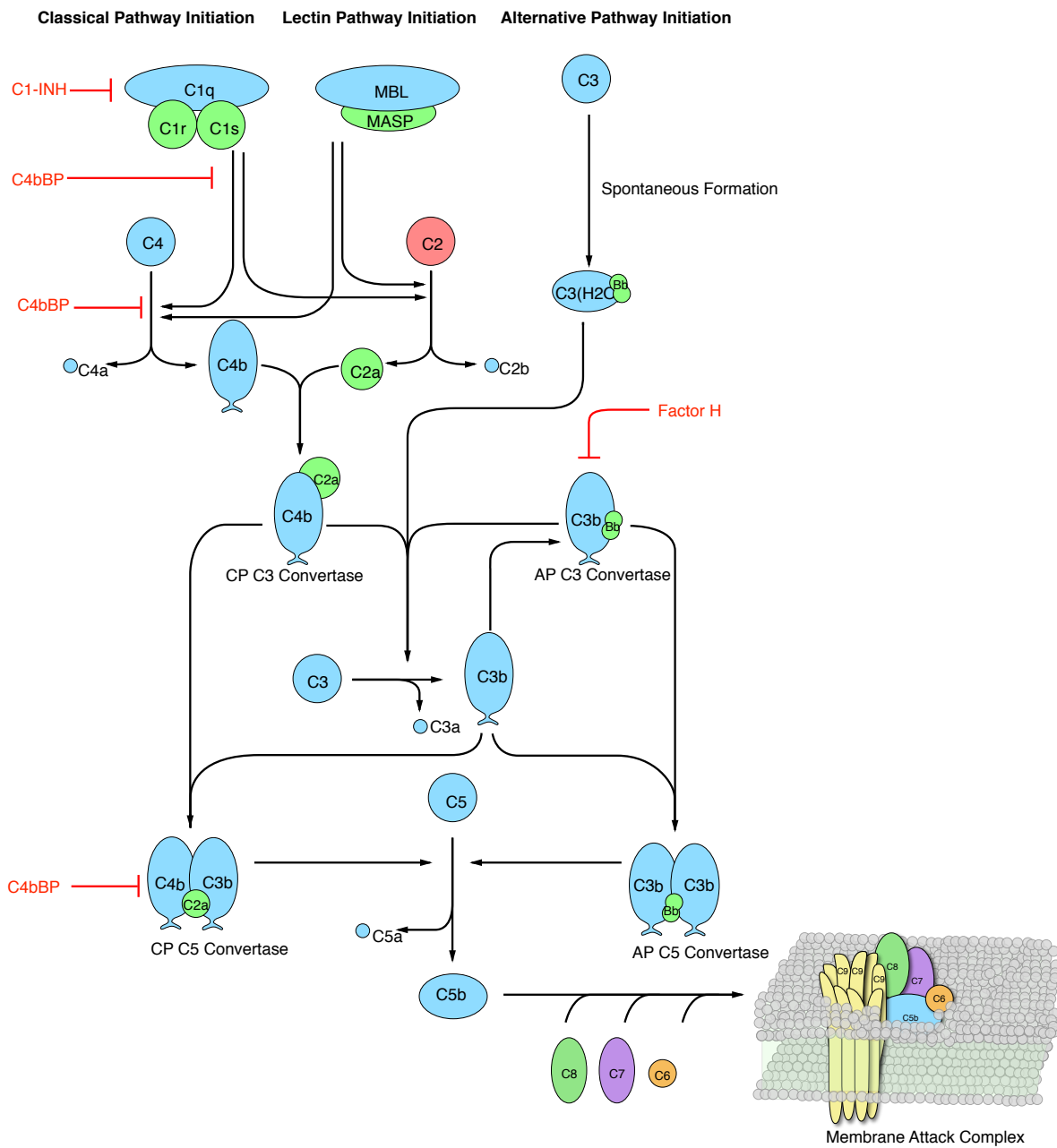


Fig. 1: Simplified schematic of the human complement system. The complement cascade is activated through any one, or more, of the three pathways: the classical, the lectin, and the alternate pathways. The classical pathway is activated by the binding of C1 complex through the C1q subunit to the IgG or IgM immune complex. This binding leads to conformational changes in the C1 complex that leads to the activation of C1r and C1s subunits. Activated C1-antibody complex cleaves C4 and C2 to form the classical C3 convertase. The lectin pathway is initiated by the binding mannose-binding lectins (MBL) and ficolins to carbohydrate moieties on the pathogen surfaces. This results in the formation mannose-binding lectin-associated serine proteases (MASPs). The MBL-MASP complex cleaves C4 and C2 to form the lectin C3 convertase. The alternative pathway is activated through a spontaneous tick-over mechanism by the hydrolysis of C3 to form fluid phase C3 convertase. The C3 convertases cleaves C3 into C3a, and C3b. C3b combines with C4b and C2a to form classical C5 convertase ($C4bC3aC3b$). The C3b binds with Factor B to form the alternate C5 convertase ($C3bBbC3b$). The C5 convertases cleave C5 into C5a, and C5b that undergoes a series of reactions to form the membrane attack complex (MAC).

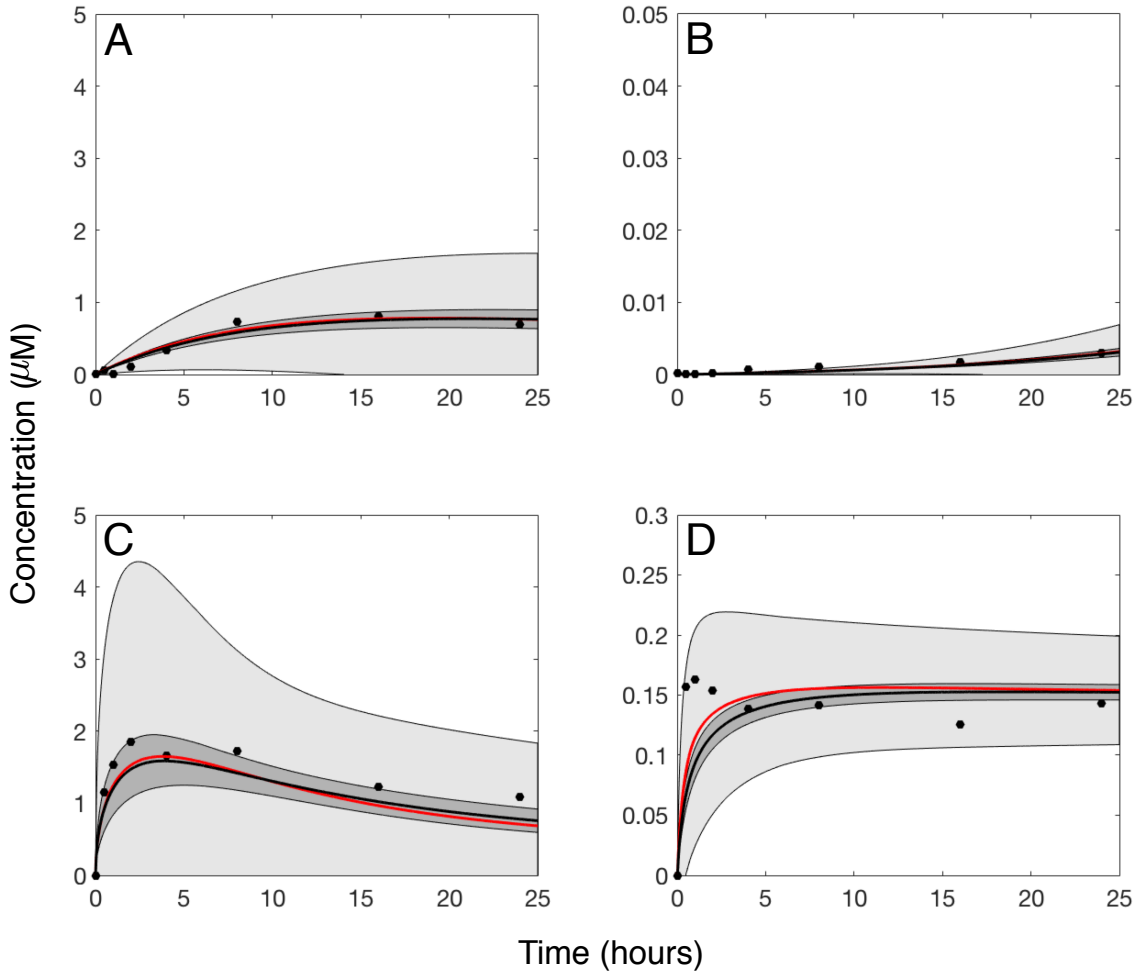


Fig. 2: Reduced order complement model training simulations. Reduced order complement model parameters were estimated using Dynamic Optimization with Particle Swarms (DOPS). The model was trained against experimental data from Shaw and co-workers [18] in the presence and absence of zymosan. The model was trained using C3a and C5a data generated from the alternative pathway (**A–B**) and lectin initiated pathway with 1g zymosan (**C–D**). The solid red line shows the simulation with the best-fit parameter, the solid black lines show the simulated mean value of C3a or C5a for 50 independent particles. The dark shaded region denotes 99 % confidence interval of the simulated mean concentrations of C3a or C5a , while the light shaded region is the 99 % confidence interval of the best prediction. All initial concentrations of complement proteins are at human serum levels unless otherwise noted.

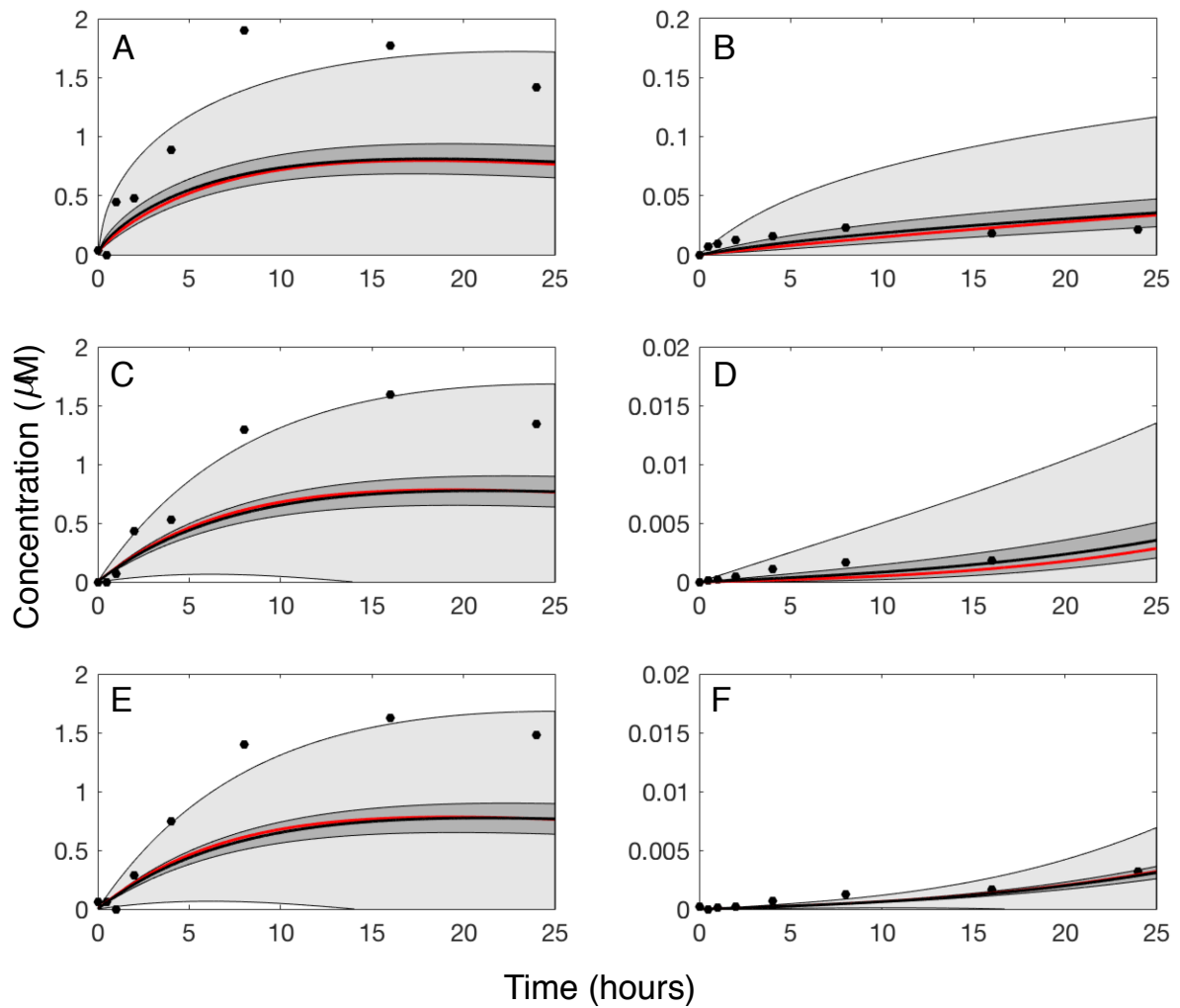


Fig. 3: Reduced order complement model predictions vs experimental data for C3a and C5a generated in the lectin pathway. The reduced order coagulation model parameter estimates were tested against data not used during model training. Simulations of C3a and C5a generated in the lectin pathway using different levels of zymosan (0.1, 0.01, and 0.001 grams of zymosan) were compared with the corresponding experimental data (A–F). The solid red line shows the simulation with the best-fit parameter, the solid black lines show the simulated mean value of C3a or C5a for 50 independent particles. The shaded region denotes 99 % confidence interval of the simulated mean concentrations of C3a or C5a, while the light shaded region is the 99 % confidence interval of the best prediction. All initial concentrations of complement proteins are at human serum levels unless otherwise noted.

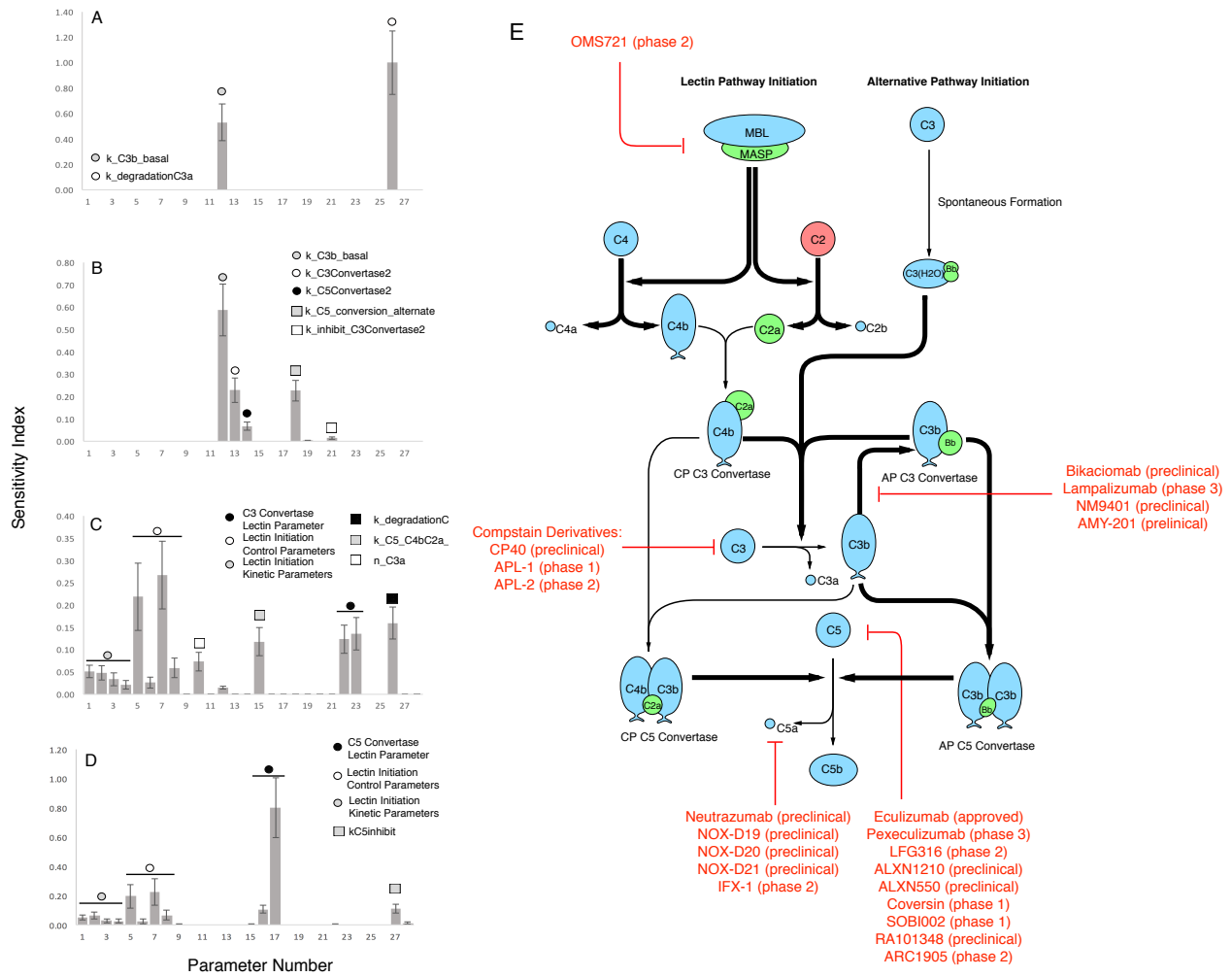


Fig. 4: Sobol's sensitivity analysis of the reduced order complement model with respect to the modeling parameters. Sensitivity analysis was conducted on the four cases we used to train our model: (A) C3a at 0g zymosan, (B) C5a 0g zymosan, (C) C3a 1g zymosan, and (D) C5a 1g zymosan. The bars denote total sensitivity index which includes local contribution of each parameter and global sensitivity of significant pairwise interactions. The error bars are the 95 percent confidence interval. Pathways controlled by the sensitivity parameters (E): Bold black lines indicates the pathway is governed by one or more sensitive parameters and the red lines shows some of the current therapeutics targets. Red indicates current complement therapeutics.

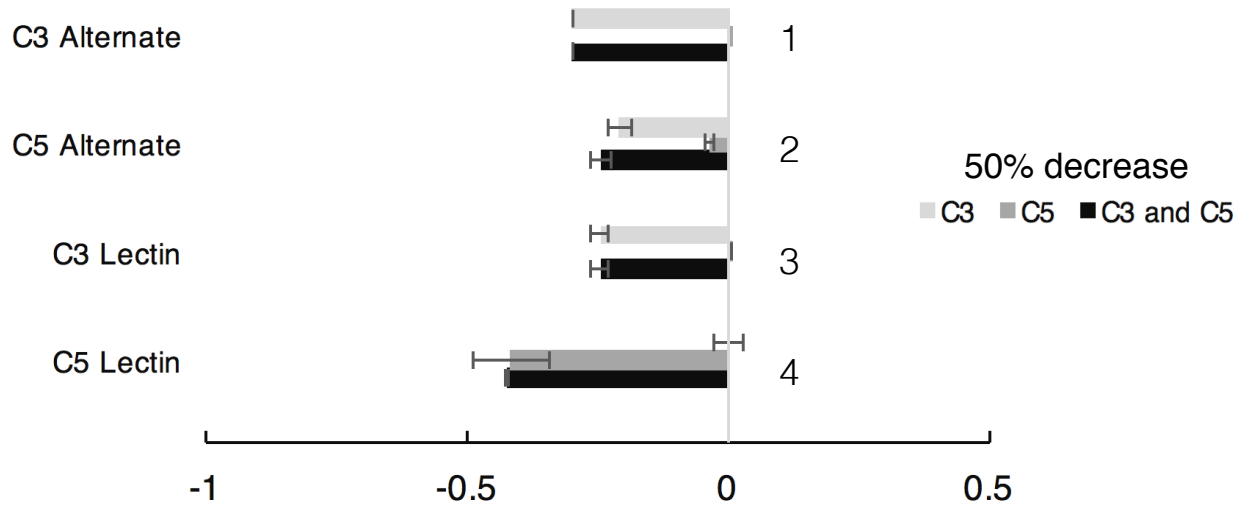
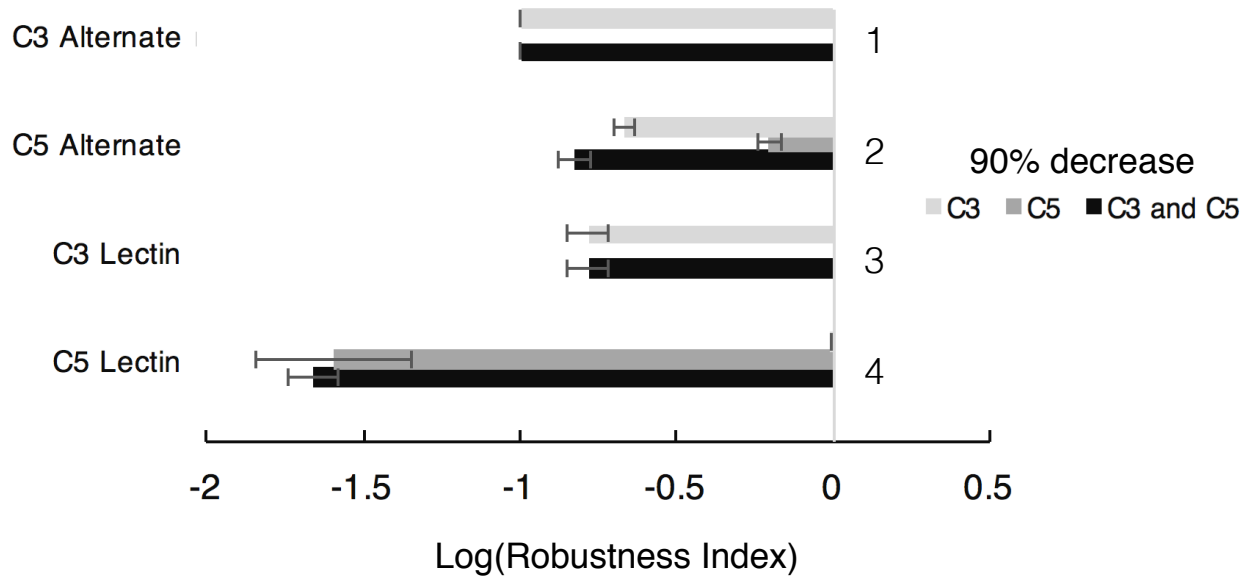
A**B**

Fig. 5: Robustness analysis of the reduced order complement model with respect to the C3 and C5 initial concentrations using 50 parameter sets. Robustness analysis was conducted on the four cases we used to train our model, C3a alternate (0 zymosan), C5a alternate (0 zymosan), C3a lectin (1 g zymosan), and C5a lectin (1 g zymosan), by reducing the initial concentration of C3 and/or C5 by (A) 50 % and (B) 90 %. The bars denote robustness index which a measure of system changes from the perturbation of initial concentration that defined by the ratio of the area under the concentration curve of perturbed case and that of the unperturbed case. The error bars represent one standard deviation. At unity, the perturbed initial concentration has no impact on the measured output, and a robustness index lesser than or greater than one indicates a negative or positive relation between the perturbed initial concentration and the measured output respectively.

548 **Supplemental materials.**

549 **Model equations.** The reduced-order complement model consisted of 18 ordinary dif-
 550 ferential equations, 12 rate equations, and two control equations:

$$\frac{dx_1}{dt} = -r_1 f_1 \quad (\text{S1})$$

$$\frac{dx_2}{dt} = -r_2 f_2 \quad (\text{S2})$$

$$\frac{dx_3}{dt} = r_1 f_1 \quad (\text{S3})$$

$$\frac{dx_4}{dt} = r_1 f_1 - r_6 \quad (\text{S4})$$

$$\frac{dx_5}{dt} = r_2 f_2 - r_6 \quad (\text{S5})$$

$$\frac{dx_6}{dt} = r_2 f_2 \quad (\text{S6})$$

$$\frac{dx_7}{dt} = r_3 - r_4 - r_5 \quad (\text{S7})$$

$$\frac{dx_8}{dt} = r_3 + r_4 + r_5 - k_{deg,c3a} * C3a \quad (\text{S8})$$

$$\frac{dx_9}{dt} = r_3 + r_4 + r_5 - r_7 \quad (\text{S9})$$

$$\frac{dx_{10}}{dt} = r_6 - r_{10} - r_8 \quad (\text{S10})$$

$$\frac{dx_{11}}{dt} = r_7 - r_{11} - r_9 \quad (\text{S11})$$

$$\frac{dx_{12}}{dt} = r_{10} - r_{14} \quad (\text{S12})$$

$$\frac{dx_{13}}{dt} = r_{10} \quad (\text{S13})$$

$$\frac{dx_{14}}{dt} = -r_{12} - r_{13} \quad (\text{S14})$$

$$\frac{dx_{15}}{dt} = r_{12} + r_{13} - k_{deg,c5a} \quad (\text{S15})$$

$$\frac{dx_{16}}{dt} = r_{12} + r_{13} \quad (\text{S16})$$

$$\frac{dx_{17}}{dt} = -r_8 - r_{14} \quad (\text{S17})$$

$$\frac{dx_{18}}{dt} = -r_9 \quad (\text{S18})$$

$$(\text{S19})$$

551 where the rate equations are given by:

$$r_1 = \frac{k_{i1}(C4)}{(K_{1s} + C4)} \quad (S20)$$

$$r_2 = \frac{k_2(C2)}{(K_{2s} + C2)} \quad (S21)$$

$$f_1 = \frac{Zymo^{\eta_1}}{(Zymo^{\eta_1} + \alpha_1^{\eta_1})} \quad (S22)$$

$$f_2 = \frac{Zymo^{\eta_2}}{(Zymo^{\eta_2} + \alpha_2^{\eta_2})} \quad (S23)$$

$$r_3 = k_3(C3) \quad (S24)$$

$$r_4 = \frac{k_4(C3C_L)(C3^{\eta_3})}{(K_{4s}^{\eta_3} + C3^{\eta_3})} \quad (S25)$$

$$r_5 = \frac{k_5(C3C_A)(C3)}{(K_{5s} + C3)} \quad (S26)$$

$$r_6 = k_6(C4b)(C2a) \quad (S27)$$

$$r_7 = k_7(C4b)(C2a) \quad (S28)$$

$$r_8 = k_8(C3C_L)(C4b)(C4BP) \quad (S29)$$

$$r_9 = k_9(C3C_A)(FactorH) \quad (S30)$$

$$r_{10} = k_{10}(C3C_L)(C3b) \quad (S31)$$

$$r_{11} = k_{11}(C3C_A)(C3b) \quad (S32)$$

$$r_{12} = \frac{k_{12}(C5C_L)(C5^{\eta_4})}{(K_{12s}^{\eta_4} + C5^{\eta_4})} \quad (S33)$$

$$r_{13} = \frac{k_{13}(C5C_A)(C5)}{(K_{13s} + C5)} \quad (S34)$$

$$r_{14} = k_{14}(C5C_L)(C4BP) \quad (S35)$$